miR-27a-3p upregulation by p65 facilitates cervical tumorigenesis by increasing TAB3 expression and is involved in the positive feedback loop of NF-κB signaling

MIN LI[1], ZIXUAN GAO[1], SHUO WANG[2], YUNGANG ZHAO[2] and HONG XIE[1]

[1]Department of Pathogen Biology, School of Basic Medical Sciences, Tianjin Medical University, Tianjin 300070; [2]Tianjin Key Laboratory of Exercise Physiology and Sports Medicine, Institute of Sport, Exercise and Health, Tianjin University of Sports, Tianjin 301617, P.R. China

Received January 18, 2023; Accepted April 4, 2023

DOI: 10.3892/or.2023.8569

Abstract. An altered microRNA (miRNA/miR)-27a-3p expression has been identified in cervical cancer, while the exact regulatory mechanisms responsible for the dysregulation of miR-27a-3p remain to be fully elucidated. In the present study, a NF-κB/p65 binding site was identified upstream of the miR-23a/27a/24-2 cluster and p65 binding enhanced the transcription of pri-miR-23a/27a/24-2, as well as the expression levels of mature miRNAs, including miR-27a-3p in HeLa cells. Mechanistically, using bioinformatics analyses and experimental validation, TGF-β activated kinase 1 binding protein 3 (TAB3) was identified as a direct target of miR-27a-3p. By binding to the 3'UTR of TAB3, miR-27a-3p significantly enhanced TAB3 expression. Functionally, it was found that the overexpression of miR-27a-3p and TAB3 promoted the malignant potential of cervical cancer cells, as evaluated using cell growth, migration and invasion assays, and specific cell marker determinations in the epithelial mesenchymal transition progression, and vice versa. Further rescue experiments revealed that the enhanced malignant effects induced by miR-27a-3p were mediated via its upregulation of TAB3 expression. Moreover, miR-27a-3p and TAB3 also activated the NF-κB signaling pathway and formed a positive feedback regulatory loop composing of p65/miR-27a-3p/TAB3/NF-κB. On the whole, the findings presented herein may provide novel insight into the underlying cervical tumorigenesis and novel biomarker identification for clinical applications.

Correspondence to: Dr Hong Xie, Department of Pathogen Biology, School of Basic Medical Sciences, Tianjin Medical University, No. 22 Qi-Xiang-Tai Road, Tianjin 300070, P.R. China
E-mail: xiehong@tmu.edu.cn

Key words: miR-27a-3p, TGF-β activated kinase 1 binding protein 3, p65, NF-κB signaling pathway, cervical cancer

Introduction

Cervical cancer is the fourth most frequently occurring cancer and the fourth leading cause of cancer-associated mortality among women, with an estimated 604,000 new cases and 342,000 related deaths worldwide in 2020 (1). Human papillomavirus (HPV) infection is a necessary, but not sufficient cause of cervical cancer. Over 100 genotypes of HPV have been identified (2), and persistent infection with high-risk HPV types (HR-HPVs) is the causal factor in >99% of cervical cancer cases and the main drivers of HR-HPV-associated oncogenesis are the oncoproteins E5, E6 and E7 (3). To date, the thinprep cytologic test (TCT) or Papanicolaou (pap) test together with HPV genotype screening programs have been applied successful and decrease the morbidity of cervical cancer in a number of countries in Europe, Oceania and North American (4,5). In addition, the HPV vaccination programs reduce the long-term future burden of cervical cancer (6,7).

MicroRNAs (miRNAs/miRs) are the most abundant class of small non-coding RNAs. They are transcribed from genomic DNA and generally processed with two endonucleases, Drosha and Dicer. miRNAs regulate gene expression at the post-transcriptional level in a sequence-dependent manner. Dysregulated miRNA expression levels have been identified in various types of cancer (8) including cervical cancer (9,10). Previously, some dysregulated miRNAs were subjected to in-depth investigations and their downstream functional mechanisms were elucidated. For example, the authors have previously performed various biochemical approaches, such as CLIP-Chip and PAR-CLIP, and identified the different targets of miR-205 and miR-944 in cervical cancer cells, respectively (11,12). Some studies have also explored the reasons for the abnormal expression of miRNAs in tumor tissues from different aspects. For example, the loss of chromosome 13q14 linked the reduced miR-15a and miR-16-1 expression in chronic lymphocytic leukemia (13). Another study demonstrated that the key transcription factor, c-Myc, resulted in the upregulated expression of the miR-17/92 cluster members due to its amplification and overexpression in multiple cancer types (14). Although studies have reported the transcriptional regulation of miRNAs from transcription

factors and epigenetic regulations (15-17), the exact regulatory mechanisms for the specific miRNA dysregulation remain to be fully elucidated.

Hsa-miR-27a-3p is located in the minus strand of human 19p13.12 and is transcribed from the same primary transcript together with miR-23a-3p/5p and miR-24-2-3p/5p, the other members of the miR-23a/27a/24-2 cluster. The abnormal expression of miR-27a has been reported in multiple cancer types and its involvement in different signaling pathways plays dual roles based on the different cell or tissue types. Previous studies have demonstrated that miR-27a-3p is involved in the PI3K/Akt pathway (18), TGF-β signaling pathway (19) and Wnt/β-catenin pathway (20,21). Recently, several long non-coding RNAs were reported to be involved in the regulatory effects of miR-27a and its mRNA target (22-24). Moreover, previous studies have linked miR-27a with the aggressive phenotypes of cervical cancer cells (25,26); however, the presented results are still controversial due to the different cell lines or the different materials used, and thus, further studies are warranted.

TGF-β activated kinase 1 binding protein 3 (TAB3) is a protein which functions in the NF-κB signaling transduction pathway (27). Together with TAB1/2 and TAK1 forming the ternary complex, TAB3 responds to the stimulation of pro-inflammatory cytokines, such as TNF-α or IL-1β, and subsequently triggers the activation of the NF-κB signaling pathway (28). TAB3 promotes the proliferation and/or invasion of various cancer cells via the activation of NF-κB signaling (29-32). For example, the TAB3/TAK1 complex directly activates STAT3 signaling via the phosphorylation of STAT3 and promotes colorectal cancer growth (29). The expression levels of TAB3 and proliferating cell nuclear antigen have been found to be gradually increased in ovarian cancer tissues and cell lines, suggesting the novel oncogenic functions of TAB3 in ovarian cancer (31). Ding *et al* (33) applied a genome-wide screening strategy and revealed that miR-195 exerted its tumor-suppressive effects via the inhibition of TAB3 and IKKα expression in hepatocellular carcinoma. However, the exact expression and functions of TAB3 in cervical cancer have not yet been reported, at least to the best of our knowledge; thus, further investigations are required.

Based on previously unpublished screening data by the authors, miR-27a-3p was one of the differently expressed miRNAs identified by silencing NFKB1. The present study thus focused on miR-27a-3p and investigated its upstream regulatory and downstream functions. The transcription factor, NF-κB subunit p65, was identified to activate the transcription of the miR-23a/27a/24-2 cluster by directly binding to the promoter region of pri-miR-23a/27a/24-2 and contributed to the upregulated expression of miR-27a-3p. Functionally, miR-27a-3p promoted the malignant potential of cervical cancer cells by increasing the colony formation rates, the migratory and invasive abilities, epithelial mesenchymal transition (EMT) and inhibiting apoptosis. Mechanistically, miR-27a-3p directly bound to the 3'UTR of TAB3 and enhanced its expression, followed by the subsequent activation of NF-κB signaling. To the best of our knowledge, this is the first functional report of TAB3 in cervical cancer cells, linking TAB3 with miR-27a-3p, and demonstrates the possible post-transcriptional regulation for TAB3 expression. The data presented herein suggest that the upregulation of miR-27a-3p expression by p65 further enhances TAB3 expression at the post-transcriptional level and sequentially mediates the activation of the NF-κB signaling pathway via TAB3 upregulation, composing of a positive feedback regulatory loop, namely the p65/miR-27a-3p/TAB3/NF-κB axis. These findings may provide novel insight into the mechanisms underlying the carcinogenesis of cervical cancer and may provide potential novel biomarkers for its management.

Materials and methods

Cells, cell culture and transfection. The human cervical cancer cell lines, HeLa (CCL-2) and C33A (HTB-31), were originally purchased from the American Type Culture Collection (ATCC) and cultured in the tumor, virus and ncRNA group. The (HeLa and C33A) cells were cultured in DMEM (VivaCell Biosciences), supplemented with 10% fetal bovine serum (FBS; Biological Industries), 100 μg/ml streptomycin and 100 IU/ml penicillin (cat. no. P1400, Beijing Solarbio Science & Technology Co., Ltd.). All cells were cultured at 37˚C with 5% CO_2.

All transfection experiments were carried out using Lipofectamine 2000® reagent (Thermo Fisher Scientific, Inc.) following the manufacturer's instructions. Plasmids (2 μg per well in a six-well plate or 500 ng per well in 24-well plate) or antisense oligonucleotides (ASO-NC/ASO-miR-27a-3p, 50 nM) were transfected into cervical cancer cells. After adding the complex (mixture of transfection reagent and DNA or ASO) to the wells, the cells were incubated at 37˚C for 24-48 h for further analyses.

Plasmid construction. The strand-specific miR-27a-3p expression vector was constructed following a previously described strategy (34). In brief, the mature miR-27a-3p sequence with its first 19 nucleotides complementary sequence and the loop sequence were synthesized and inserted into the pcDNA3-U6M2 vector (modified from the pcDNA3 vector, replacing the CMV promoter with U6 promoter, abbreviated as U6M2; a gift from Dr Per Johansson, Karolinska Institutet, Sweden) between the *Bgl*II/*Kpn*I sites. For miR-27a-3p inhibition, the synthesized 2'-O-methyl-modified antisense oligonucleotides of miR-27a-3p (ASO-miR-27a-3p) and the scramble control oligonucleotides (ASO-NC) were purchased from Shanghai GenePharma Co., Ltd.

To construct the overexpression vector for TAB3, the full coding sequence of TAB3 from the cDNA of HeLa cells was amplified and cloned into the pcDNA3-3xFlag vector (a modified vector, named as pcDNA3/Flag-KBE, abbreviated as KBE, since the 3xFlag sequences inserted between the *Nco*I/*Kpn*I sites, the cloned fragment can only be inserted downstream of the *Kpn*I site) between the *Kpn*I/*Eco*RI sites, respectively. The overexpression vectors for p65 (KBE-p65), p50 (KBE-p50) were provided by Dr Weiying Liu (Tianjin Medical University), the shRNA vector targeting NFKB1 and the empty vector control pSilencer2.1-U6 neo were provided by Dr Qi Sun (Tianjin Medical University). The shRNA vectors targeting TAB3, NF-κB/p65 and Agonaute (AGO)2 (shR-TAB3, shR-p65, shR-AGO2) were constructed by annealing the

synthesized oligonucleotides into pcDNA3-U6M2 vector between the *Bgl*II/*Kpn*I sites.

The luciferase reporter vectors for the miR-27a promoter were constructed by amplifying the respected sequences from the genomic DNA of HeLa cells and cloned into the pGL3-enhancer vector (Promega Corporation), between the *Xho*I/*Hin*dIII sites (pGL3-P1 and pGL3-P2). The series truncated promoter reporter vectors (R175, R259, R509, F259 and F509) were constructed using the same strategy by amplifying the related fragments from the pGL3-P2 plasmid. The mutated reporter vector with the p65 binding site deletion (F509-Del546) was synthesized by Sangon Biotech Co., Ltd.

The wild-type and the mutated form of the 3'UTR EGFP reporter vectors for TAB3, mitogen-activated protein kinase kinase kinase 14 (MAP3K14) and TNF receptor associated factor 3 (TRAF3) were constructed by annealing the synthesized oligonucleotides (containing the predicted miR-27a-3p binding sites, wild-type and mutated form) and cloning into the pcDNA3/EGFP vector between the *Bam*HI/*Eco*RI sites. All constructed vectors were verified using Sanger sequencing at GENEWIZ. All primers used for PCR amplification and all oligonucleotides for preparing constructs were synthesized by Synbio Technologies or General Biol, and their sequences are listed in Supplementary Table SI.

Bioinformatics analyses. The online miRNA target prediction tool, TargetScan (https://www.targetscan.org/), was used to predict the potential targets of miR-27a-3p. An online analyses tool (Assistant for Clinical Bioinformatics, https://www.aclbi.com) based on The Cancer Genome Atlas (TCGA)-Cervical Squamous Cell Carcinoma and Endocervical Adenocarcinoma (CESC) dataset (http://portal.gdc.cancer.gov) was used to analyze the expression levels of miRNAs and the selected potential targets. The NCBI GEO datasets (GSE86100 and GSE20592) were also selected to analyze the expression levels of miR-27a-3p and the miR-23a/27a/24-2 cluster members. GEPIA2 (http://gepia2.cancer-pku.cn/#index) was used to analyze the overall and disease-free survival based on the expression levels of TAB3, MAP3K14 and TRAF3 from the TCGA-CESC dataset, and the online tool HIPLOT (https://hiplot.com.cn/cloud-tool/drawing-tool/detail/122) was applied to draw the survival curves based on miR-27a-3p expression from the TCGA-CESC dataset.

For promoter prediction, with the help of FANTOM (https://fantom.gsc.riken.jp/) and Promoter 2.0 (https://services.healthtech.dtu.dk/service.php?Promoter-2.0) predictions, combining with CpG island analysis, the upstream (~8 kb) sequences of miR-27a-3p were analyzed.

RNA extraction and reverse transcription-quantitative PCR (RT-qPCR). Total RNA was extracted from the cultured cells using TRIzol® reagent (Invitrogen; Thermo Fisher Scientific, Inc.) following the manufacturer's recommendations. The concentration of the RNA was measured using a NanoDrop 2000 spectrophotometer (Thermo Fisher Scientific, Inc.) and stored at -80˚C. cDNA was synthesized using the HiScript II Q Select RT SuperMix for qPCR kit (cat. no. R233-01, Nanjing Vazyme Biotech Co., Ltd.). A total of 1 μg RNA was first treated by genome DNA wiper mix at 42˚C for 2 min and followed by 50˚C/15 min plus 85˚C/5 sec for cDNA synthesis. The expression levels of miRNAs and mRNAs were quantified by qPCR using 2X Universal SYBR-Green fast qPCR Mix (ABclonal Biotech Co., Ltd.). β-actin and U6 snRNA were used as the endogenous controls for mRNA and miRNA quantification, respectively, reported as $2^{-\Delta CCq}$ (35) and further normalized to their respective controls. All primers used for RT-qPCR were synthesized by Synbio Technologies and are listed in Supplementary Table SI.

Western blot analyses. Cells were collected after 48 h post-transfection and lysed in RIPA buffer (cat. no. R0010, Beijing Solarbio Science & Technology Co., Ltd.). Proteins (50-100 μg per lane, determined using the BCA protein assay kit, Beyotime Institute of Biotechnology, Inc.), were separated by 10% SDS-PAGE and transferred to nitrocellulose membranes. After blocking with 5% non-fat milk in 1xTBST (cat. no. BF-0113, Beijing Dingguo Biotechnology Co. Ltd.) at room temperature for 2 h, followed by incubation with the indicated dilutions of the primary antibodies overnight at 4˚C. GAPDH served as the endogenous loading control for the whole cell lysates and the cytoplasmic sub-fractions, and Lamin B1 was selected for the internal reference index for the nuclear fractions. After washing three times (5 min for each) with TBST, the secondary antibodies (anti-mouse or anti-rabbit IgG-HRP) were added and incubated for a further 1 h at room temperature. Detection was performed using ECL HRP chemiluminescent substrate reagent (cat. no. BL520B, Biosharp Life Sciences). The protein expression levels were quantified on the blots using ImageJ software (version 1.52v, National Institutes of Health). All antibodies used in the present study are listed in Table I.

Luciferase promoter reporter and EGFP 3'UTR reporter analyses. For promoter luciferase reporter assays, the HeLa cells were seeded in 96-well plates and transfected with the indicated series reporter vectors (100 ng/well) with/without the modulation of NF-κB/p65 or NFKB1/p50. Each well was co-transfected with the pRL-CMV vector (10 ng/well) for normalization. The activities of luciferases (Firefly and *Renilla*, FL and RL) were measured at 30 h post-transfection using the Dual-Luciferase Assay kit (cat. no. E1910, Promega Corporation) following the recommendations of the manufacturer. The relative Firefly activities were normalized to the *Renilla* luciferase activities in each well.

For 3'UTR EGFP fluorescence reporter assays, the HeLa cells were seeded in 24-well plates and transfected with the wild-type or mutated form of the reporter vectors (500 ng/well) with/without the overexpression of miR-27a-3p. pDsRed2-N1 (100 ng/well, Clontech; Takara Bio USA) co-transfected into each well for normalization. At 48 h following transfection, the cells were lysed with RIPA buffer and the fluorescence intensities of EGFP and RFP were determined using a microplate reader (Tecan Spark, Tecan Group, Ltd.).

Colony formation assays. Following 24 h of transfection, the HeLa and C33A cells were re-suspended and seeded in a 24-well plate (300 cells/well) or 12-well plate (500 cells/well) and incubated for a further 10-14 days a 37˚C in a 5% CO_2 incubator. During the incubation period, fresh culture medium

Table I. The detailed information for all the antibodies used in the present study.

Primary antibodies				
Antibody	Manufacturer	Cat. no.	Species	Dilution
TAB3	Tianjin Saier Biotechnology Co., Ltd.	SRP08919	Rabbit	1:500 (WB)
Cleaved PARP	Beyotime Institute of Biotechnology	AF1567	Rabbit	1: 1,000 WB)
Vimentin	Beyotime Institute of Biotechnology	AF0318	Mouse	1:3,000 (WB)
EpCAM	Chengdu Zen Bioscience Co., Ltd.	R24219	Rabbit	1:1,000 (WB)
Flag	Beyotime Institute of Biotechnology	AF519	Mouse	1:1,000 (WB)
Agonaute 2	Chengdu Zen Bioscience Co., Ltd.	R23523	Rabbit	1:1,000 (WB)
MAP3K14	Tianjin Saier Biotechnology Co., Ltd.	SRP06501	Rabbit	1:500 (WB)
TRAF3	Wanleibio Co., Ltd.	WL04574	Rabbit	1:250 (WB)
GAPDH	Beyotime Institute of Biotechnology	AF1186	Rabbit	1:10,000 (WB)
Lamin B1	Tianjin Saier Biotechnology Co., Ltd.	SRP13156	Rabbit	1:3,000 (WB)
NF-κB/p65	Beyotime Institute of Biotechnology	AF1234	Rabbit	1:1,000 (WB)
NF-κB/p65	Beyotime Institute of Biotechnology	AF1234	Rabbit	1:200 (IF)
Secondary antibodies used for western blot analysis and immunofluorescence				
Goat anti-mouse IgG-HRP	Boster Biological Technology Co., Ltd.	BA1050	Goat	1:80,000 (WB)
Goat anti-rabblit IgG-HRP	Boster Biological Technology Co., Ltd.	BA1054	Goat	1:80,000 (WB)
Goat anti-rabbit IgG-FITC	Tianjin Sungene Biotech Co., Ltd.	AJ1027	Goat	1:200 (IF)

WB, western blot analysis; IF, immunofluorescence; TAB3, TGF-β activated kinase 1 binding protein 3; TRAF3, TNF receptor associated factor 3; MAP3K14, mitogen-activated protein kinase kinase kinase 14.

was changed every 3-4 days. The cells were fixed with 4% paraformaldehyde (cat. no. P1110; Beijing Solarbio Science & Technology Co., Ltd.) for 30 min and stained with 0.5% crystal violet (cat. no. C0121, Beyotime Institute of Biotechnology) for 10 min at room temperature, and the colonies including >50 cells were counted using a light microscope (ECLIPSE TS100, Nikon Corporation).

Transwell migration and invasion assays. Cell migration and invasion were analyzed using 24-well Boyden chambers with an 8-μm pore size polycarbonate membrane. The insert chambers were placed in a 24-well plate, containing 800 μl culture medium with 30% FBS. For the invasion assays, the Matrigel (cat. no. 356234, Corning Inc.) was 1:7 diluted with cold serum-free medium, placed onto the chamber membrane in advance and incubated at 37˚C for at least 2 h. In brief, following 24 h of transfection, $6x10^5$ cells (for migration) or $8x10^5$ cells (for invasion) were re-suspended in serum-free culture medium and seeded in the upper chamber and incubated at 37˚C for a further 36 h. At the end of the incubation period, the non-migrated or non-invaded cells on the top surface of membrane were removed using cotton swabs, and the migrated or invaded cells on the bottom surface of membrane were fixed with 4% paraformaldehyde for 30 min and stained with crystal violet for 10 min at room temperature. For quantification, the stained migrated or invaded cells were dissolved using 33% acetic acid reagent and the optical densities at 570 nm were determined using an MQX200 microplate reader (BioTek Instruments, Inc.).

Immunofluorescence analysis. The HeLa cells were seeded in a 12-well plate with coverslips inside. Following transfection with 1 μg plasmids (miR-27a-3p, TAB3 and their respective vector controls) for 48 h, the cells were fixed with 4% paraformaldehyde for 10 min at room temperature, permeabilized with 0.01% Triton X-100 (v/v, in 1X PBS) for 2 min, and blocked in 10% donkey serum (cat. no. S9100, Beijing Solarbio Science & Technology Co., Ltd.) at room temperature for 30 min. Following overnight incubation with anti-p65 antibody (1:200; cat no. AF1234, Beyotime Institute of Biotechnology) at 4˚C, the FITC-labeled secondary antibody (1:200; cat. no. AJ1027, Tianjin Sungene Biotech Co., Ltd.) were added and incubated for 2 h at 4˚C in the dark. The cells were mounted with DAPI Fluoromount-G and images were captured using a TS2 fluorescence microscope (Nikon Corporation). ImageJ software (version 1.52v, National Institutes of Health) was used to analyze the mean fluorescence intensities from at least three views, including ~15-25 individual cells, and the quantification was normalized to their respective control groups.

Cell cytosolic and nuclear fraction extraction. At 48 h post-transfection, the cells (in a six-well plate) were trypsinized, harvested with cold PBS and lysed with 150 μl Buffer I [0.4% NP-40 (cat. no. DH218 (Guangzhou Dingguo Biology) in PBS with 1X Protease Inhibitor Cocktail, cat. no. P6730, Beijing Solarbio Science & Technology Co., Ltd.] by vortexing. Following incubation for 5 min at 4˚C, the lysates were centrifuged at 5,000 x g for 10 min at 4˚C. The supernatant (i.e., the cytosolic extracts) was carefully collected and stored at

-20˚C for further analyses. The precipitates were re-suspended in 100 μl Buffer II (0.1% NP-40 in PBS with 1X Protease Inhibitor Cocktail) by gently pipetting up and down, followed by centrifugation at 5,000 x g for 10 min at 4˚C. The supernatants were discarded and the precipitates were dissolved in 100 μl RIPA buffer (cat. no. R0010, Beijing Solarbio Science & Technology Co., Ltd.) and incubated at -80˚C for 30 min; these were the nuclear extracts used for further analyses.

Statistical analyses. All experiments were performed at least in triplicate independently. All data were expressed as the mean ± SEM and were analyzed using GraphPad Prism 7 (GraphPad Software, Inc.). The significance of the differences between two or multiple groups was evaluated using an unpaired Student's t-test or one-way ANOVA followed by a Tukey's post hoc test. The paired Student's t-test was only applied with the GSE20592 dataset. $P \leq 0.05$ was considered to indicate a statistically significant difference. Pearson's correlation test was applied to analyze the correlation between the miR-27a-3p and TAB3 expression levels.

Results

The high expression of miR-27a-3p facilitates the malignant properties and enhances the nuclear translocation of NF-κB/p65 in cervical cancer cells. To investigate the expression levels of miR-27a-3p and the other members from miR-23a/27a/24-2 cluster in cervical cancer tissues, expression analyses were performed based on the GSE86100, GSE20592 and TCGA-CESC datasets. As demonstrated in Figs. 1A and S1, the expression of miR-27a-3p was significantly higher in cervical cancer tissues compared with normal tissues, while the expression levels of the other miRNAs were not consistent. Further RT-qPCR analyses were first applied to investigate the effectiveness of the constructed miR-27a-3p strand specific expression vector and the synthesized ASO-miR-27a-3p. As shown in Fig. 1B, the stand-specific miR-27a-3p construct enhanced and ASO-miR-27a-3p decreased the expression of miR-27a-3p in HeLa cells. Subsequently, gain- and loss-of-function experiments were performed to investigate its multiple effects on cell malignancies. The overexpression of miR-27a-3p significantly enhanced the colony formation rates of cervical cancer cells, while the inhibition of miR-27a-3p resulted in decreased colony formation rates in both the HeLa and C33A cells (Fig. 1C). Moreover, miR-27a-3p overexpression inhibited the apoptosis of cervical cancer cells, since the expression of cleaved PARP (89 kDa) increased upon miR-27a-3p inhibition and decreased with the overexpression of miR-27a-3p (Fig. 1D).

Furthermore, the expression levels of different biomarkers in the epithelial-mesenchymal transition (EMT) processes were examined using western blot analyses. As shown in Fig. 1E, the expression of the epithelial cell marker, EpCAM, decreased and that of the mesenchymal cell marker, Vimentin, increased with the overexpression of miR-27a-3p, and vice versa. Transwell migration and invasion assays were used to evaluate the effects of miR-27a-3p in cervical cancer cells. The ectopic expression of miR-27a-3p significantly enhanced the migratory (upper panel) and invasive (lower panel) abilities of the HeLa and C33A cells, and the inhibition of miR-27a-3p significantly decreased the migration and invasion of cervical cancer cells (Fig. 1F). Taken together, these results indicate the cancer-promoting effects of miR-27a-3p in cervical cancer cells.

Since miR-27a-3p was identified as one of the differentially expressed miRNAs associated with NF-κB silencing in previous unpublished screening data by the authors, in the present study, western blot and immunofluorescence analyses were performed to examine the effects of miR-27a-3p on nuclear p65 expression and the potential activation of NF-κB signaling. The sub-fraction extracts examined using western blot analysis revealed the increased nuclear p65 and decreased cytoplasmic p65 expression levels upon the overexpression of miR-27a-3p in the HeLa and C33A cells, and the opposite results were obtained following the inhibition of miR-27a-3p expression (Fig. 1G). The enhanced nuclear p65 signals upon miR-27a-3p overexpression were also observed in the HeLa cells, as evaluated using immunofluorescence analyses (Fig. 1H and I). Further RT-qPCR assays were performed to evaluate the expression levels of NF-κB-dependent genes, such as VEGFB, c-Myc and cyclin D1 upon miR-27a-3p modulation. As shown in Fig. 1J, the mRNA expression levels of VEGFB, c-Myc and cyclin D1 were significantly enhanced/decreased by miR-27a-3p overexpression/inhibition in HeLa cells. Taken together, these data suggest that the enhanced p65 nuclear translocation and the activation of NF-κB signaling are induced by miR-27a-3p overexpression.

TAB3 is upregulated by miR-27a-3p via directly binding to its 3'UTR. To further investigate the regulatory mechanisms of miR-27a-3p and its possible connections with the NF-κB signaling pathway, bioinformatics analyses were first performed to search for its potential targets and focused on the molecules involved in NF-κB signaling. TAB3, MAP3K14 and TRAF3 were first selected for verification using the 3'UTR EGFP fluorescence reporter systems. As shown in Fig. 2A, there was a putative miR-27a-3p binding site in the position 368-390 of 3'UTR of TAB3. When the miR-27a-3p expression vector and the wild-type 3'UTR reporter vector were co-transfected, the normalized EGFP intensities were significantly increased, while the mutant 3'UTR reporter vector co-transfection abolished the enhancement of EGFP intensities induced by miR-27a-3p, suggesting the direct binding of miR-27a-3p with the 3'UTR of TAB3. Further western blot and RT-qPCR analyses revealed the increased TAB3 expression at both the protein and mRNA level upon miR-27a-3p overexpression, and the decreased TAB3 expression upon miR-27a-3p inhibition using ASO-miR-27a-3p in HeLa and C33A cells (Fig. 2B). Further correlation analyses based on the available TCGA-CESC dataset including 303 cervical cancer tissues revealed a significant positive correlation between miR-27a-3p and TAB3 expression levels (Fig. 2C).

Similarly, bioinformatics analyses also revealed the putative miR-27a-3p binding sites present in the 3'UTRs of MAP3K14 (position:1245-1267) and TRAF3 (position:1613-1635), as presented in Fig. S2A. The 3'UTR EGFP fluorescence reporter analyses obtained the similar results as TAB3, i.e., the increased EGFP intensities were induced by miR-27a-3p overexpression, and this enhancement was abolished by co-transfection with

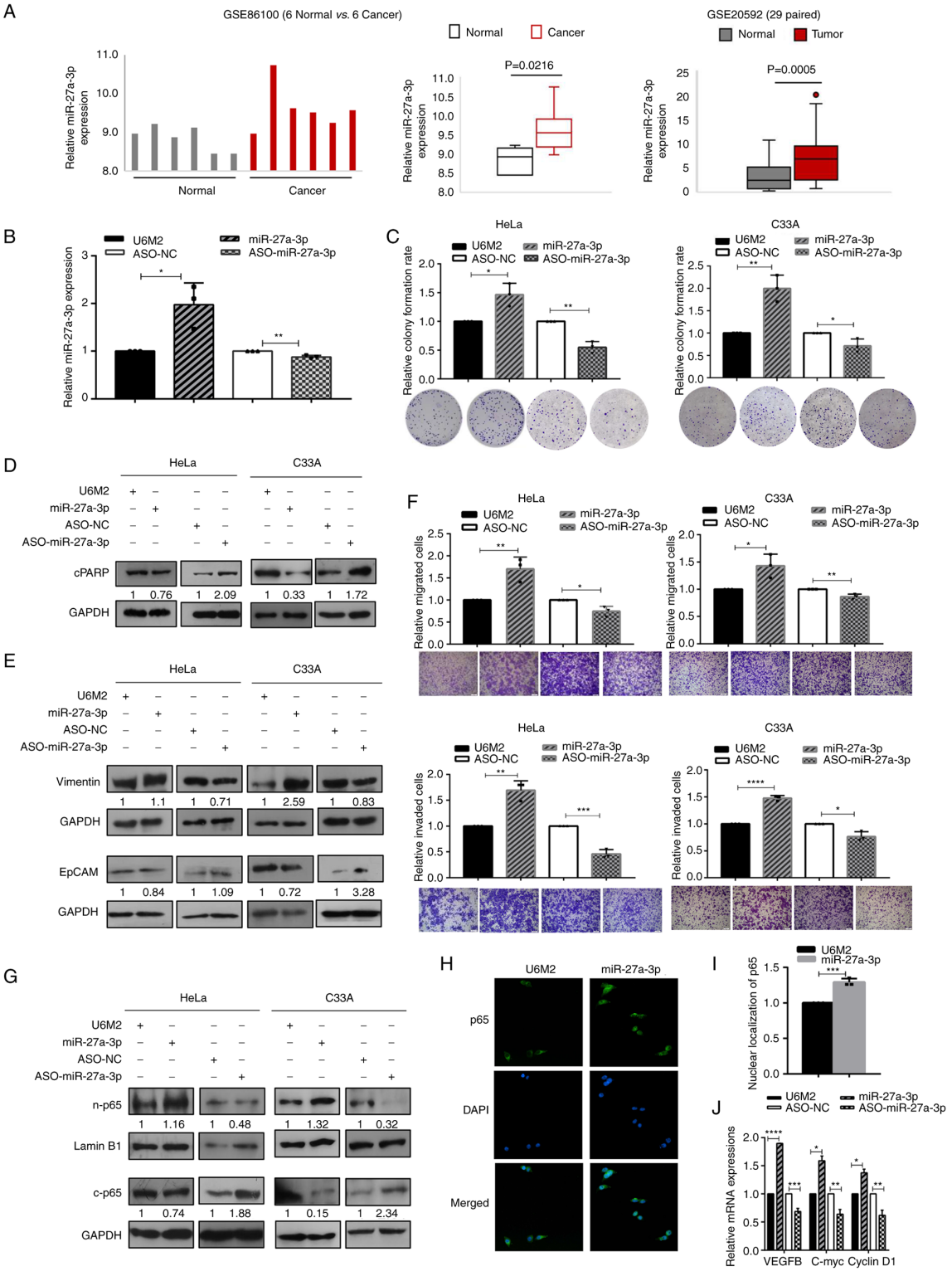

Figure 1. The high expression of miR-27a-3p facilitates the malignant properties and enhances the nuclear translocation of NF-κB/p65 in cervical cancer cells. (A) miR-27a-3p was highly expressed in cervical cancer tissues compared with normal tissues based on the GSE86100 and GSE20592 datasets. (B) RT-qPCR assays were used to determine the effectiveness of miR-27a-3p overexpression and inhibition in HeLa cells. (C) The effects of miR-27a-3p on cell growth were evaluated using colony formation assays in cervical cancer cells. (D) The expression of cleaved PARP (as an indicator of cell apoptosis) was examined using western blot analysis upon the modulation of miR-27a-3p expression in cervical cancer cells. (E) Western blot analysis was performed to determine the specific biomarkers (Vimentin for mesenchymal cells, and EpCAM for epithelial cells) in the epithelial mesenchymal transition process in cervical cancer cells upon miR-27a-3p overexpression and inhibition. (F) The effects of miR-27a-3p on migration (upper panel) and invasion (lower panel) were determined using Transwell assays in cervical cancer cells; scale bars, 100 μm. (G) Western blot analysis of sub-fraction extracts presented the nuclear and cytoplasmic p65 expression upon the modulation of miR-27a-3p expression in cervical cancer cells. (H) Representative images of immunofluorescence assays indicated the enhanced nuclear translocation of p65 upon miR-27a-3p overexpression in HeLa cells (magnification, x400). (I) The quantification of nuclear p65 expression based on immunofluorescence assays. (J) RT-qPCR assays were performed to determine the expression of NF-κB dependent genes upon the modulation of miR-27a-3p expression. (C and F) The raw representative graphs of the stained cells are presented under the quantitative histograms. (D, E and G) The numbers under the western blot bands indicate the relative quantifications, as normalized to their endogenous loading control, respectively. *P<0.05, **P<0.01, ***P<0.001 and ****P<0.0001, vs. their respective control group. RT-qPCR, reverse transcription-quantitative PCR.

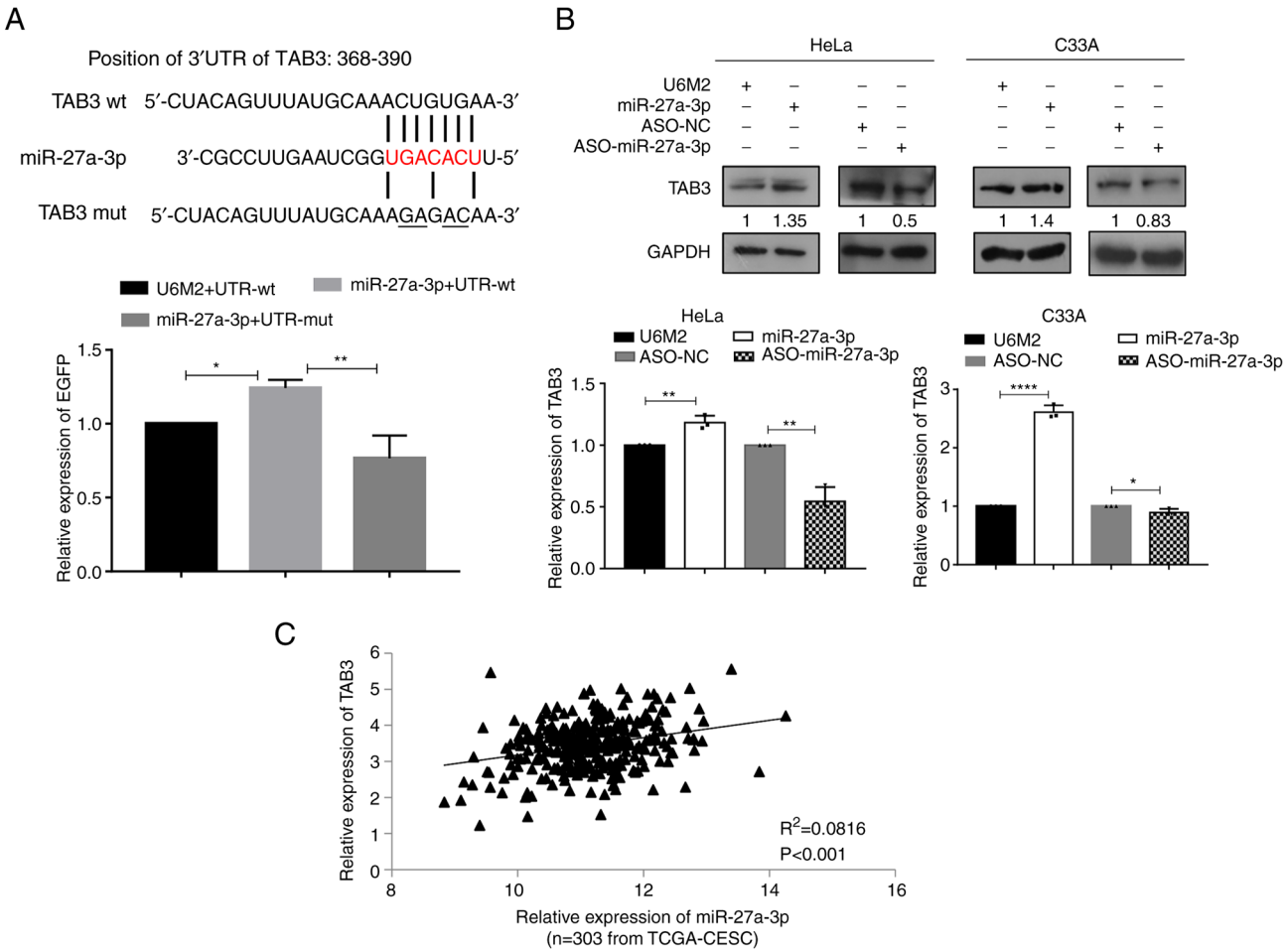

Figure 2. TAB3 expression is upregulated by miR-27a-3p via the direct binding to its 3'UTR. (A) The upper panel presents the sequence alignment of miR-27a-3p with the wild-type (wt) and the mutated (mut, in bold font and underlined) 3'UTR of TAB3. The seed sequence of miR-27a-3p is indicated in red characters. The lower panel presents the effects of miR-27a-3p on the EGFP intensities using EGFP reporter systems. (B) Western blot analysis (upper panel) and reverse transcription-quantitative PCR (lower panel) assays determined the effects of miR-27a-3p on the expression of TAB3 in cervical cancer cells. The numbers under the western blot bands indicate the relative quantifications, as normalized to their endogenous loading control. (C) The expression levels of TAB3 and miR-27a-3p positively correlated based on the available 303 cervical cancer tissues from TCGA-CESC dataset. *P<0.05, **P<0.01 and ****P<0.0001, vs. their respective control group. TAB3, TGF-β activated kinase 1 binding protein 3; TCGA-CESC, The Cancer Genome Atlas (TCGA)-Cervical Squamous Cell Carcinoma and Endocervical Adenocarcinoma (CESC).

the mutated 3'UTR reporter vectors (Fig. S2B). The MAP3K14 and TRAF3 expression levels were also analyzed upon the modulation of miR-27a-3p expression in cervical cancer cells. As shown in Fig. S2C, the mRNA expression levels of MAP3K14 and TRAF3 were significantly increased following miR-27a-3p overexpression and decreased upon miR-27a-3p inhibition in both cervical cancer cells, and enhanced protein expression levels were also observed upon the ectopic expression of miR-27a-3p in HeLa cells (Fig. S2D). Further survival analyses based on the expression levels of TAB3, MAP3K14, TRAF3 and miR-27a-3p from the TCGA-CESC dataset were conducted using online tools. As illustrated in Fig. S3, only MAP3K14 expression was associated with significant changes in the overall survival of patients; i.e., patients with a higher MAP3K14 expression exhibited an improved survival rate; however, no significant associations were found between TAB3, TRAF3 and miR-27a-3p expression and patient survival.

To further investigate the mechanisms responsible for the promoting effects on TAB3 expression induced by miR-27a-3p, the present study first determined whether AGO2 protein participated in this process. By constructing shRNA vectors for AGO2 (shR1-AGO2 and shR2-AGO2) and determining their efficiencies (Fig. S4A), miR-27a-3p was overexpressed in C33A cells with/without shR-AGO2 and the protein expression levels of TAB3 were re-evaluated. As demonstrated in Fig. S4B, a similar upregulated TAB3 expression was observed upon miR-27a-3p overexpression with the inhibition of AGO2, indicating that AGO2 was involved in the upregulation of TAB3 induced by miR-27a-3p. Notably, the globally decreased TAB3 protein expression was also observed upon the silencing of AGO2 compared with the control group, suggesting the potential regulation of TAB3 by other AGO2-associated mechanisms or other AGO2-dependent miRNA regulations.

TAB3 contributes to the malignant phenotypes of human cervical cancer cells. Overexpression and knockdown vectors were constructed for TAB3 (KBE-TAB3, shR1-TAB3 and shR2-TAB3) for the further investigation of its biological roles. Firstly, their efficiencies were evaluated using western blot analyses with anti-TAB3 and anti-Flag. As shown in Fig. 3A,

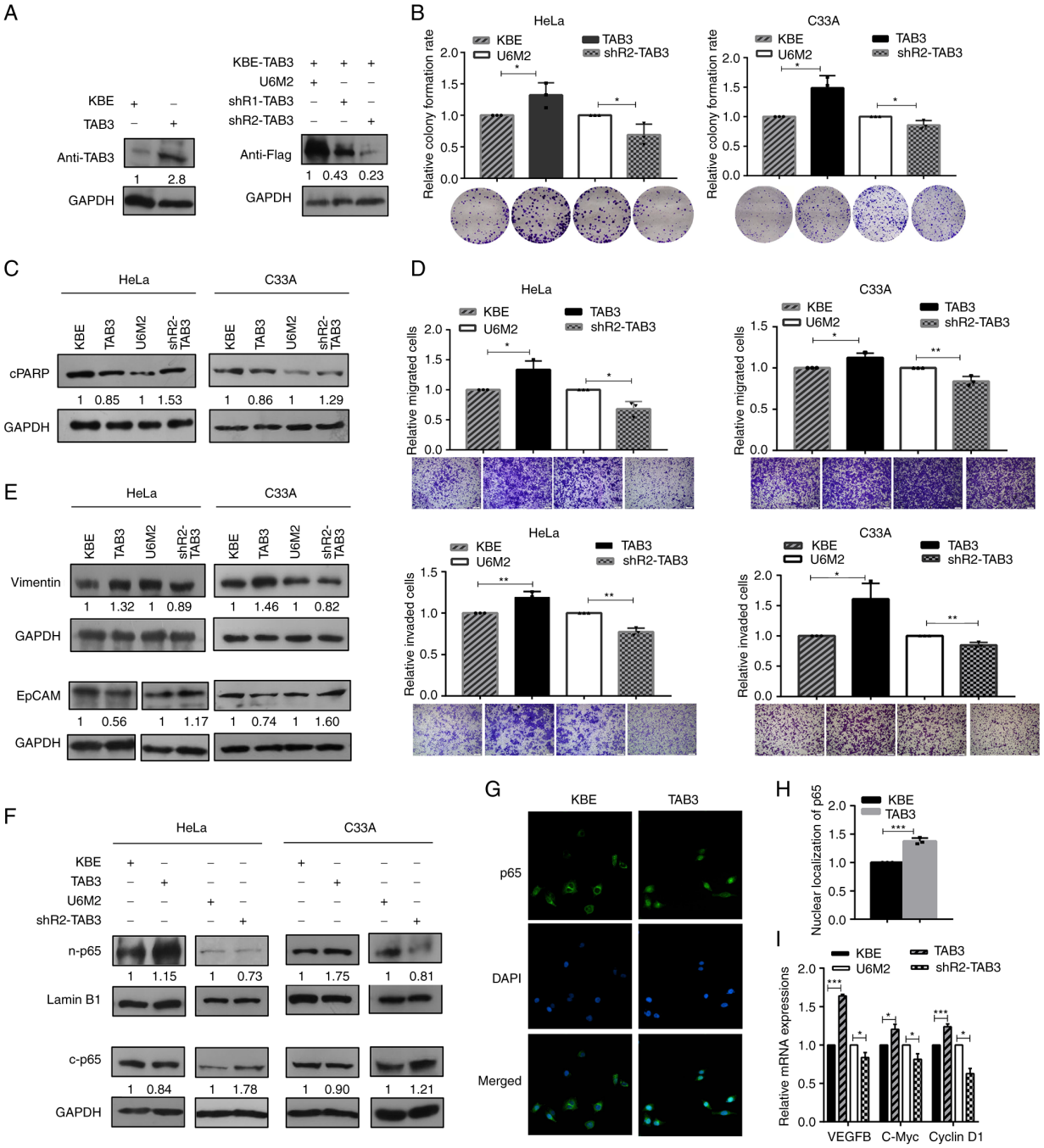

Figure 3. TAB3 contributes to the malignant phenotypes of human cervical cancer cells. (A) The efficiencies of the constructed TAB3 overexpression and inhibition vectors (KBE-TAB3, abbreviated as TAB3, and shRNA vectors, indicated as shR1-TAB3 and shR2-TAB3) were evaluated using western blot analysis. (B) Colony formation assays were performed to evaluate the effects of TAB3 modulation on cell growth. (C) Representative western blots of cleaved PARP illustrating the effects of TAB3 overexpression and inhibition on apoptosis. (D) Transwell migration (upper) and invasion (lower) assays were applied to determine the effects of the modulation of TAB3 expression; scale bars, 100 μm. (E) The specific biomarkers (Vimentin and EpCAM) of the epithelial-mesenchymal transition process were determined using western blot analysis to investigate the effects of TAB3 overexpression and inhibition. (F) Western blot analysis indicated the increased nuclear p65 and decreased cytoplasmic p65 expression upon the ectopic expression of TAB3 in cervical cancer cells, and vice versa. (G) Representative images of immunofluorescence assays indicated the enhanced nuclear translocation of p65 upon TAB3 overexpression in HeLa cells (magnification, x400). (H) The quantification of nuclear p65 expression based on immunofluorescence assays. (I) Reverse transcription-quantitative PCR assays were performed to determine the expression of NF-κB-dependent genes (VEGFB, C-Myc and cyclin D1) upon the modulation of TAB3 expression. (B and D) The raw representative graphs of the stained cells are presented under the quantitative histograms. (A, C, E and F) The numbers under the western blot bands indicate the relative quantifications, as normalized to their endogenous loading control, respectively. All experiments, apart from those in (A) (n=2) were performed at least three times independently. *P<0.05, **P<0.01 and ***P<0.001, vs. their respective control group. TAB3, TGF-β activated kinase 1 binding protein 3.

the KBE-TAB3 vector efficiently enhanced TAB3 expression, and both the shR1-TAB3 and shR2-TAB3 vectors inhibited TAB3 expression. The shR2-TAB3 vector was selected for performing the further loss-of-function experiments, since its silencing effect was more prominent than that of shR1-TAB3. By gain- and loss-of-function transit transfection, the series

functional effects of TAB3 on the colony formation, apoptosis, migration and invasion of cervical cancer cells, as well as the expression levels of EMT-associated biomarkers were determined. The results revealed increased colony formation rates upon TAB3 overexpression in cervical cancer cells, and TAB3 inhibition using shRNA significantly decreased the colony formation abilities (Fig. 3B). The decreased expression of cleaved PARP upon TAB3 overexpression and the enhanced expression of cleaved PARP following the silencing of TAB3 expression were observed using western blot analyses in the cervical cancer cells (Fig. 3C).

Transwell migration and invasion assays revealed the elevated migration (upper panel) and invasion (lower panel) properties following the ectopic expression of TAB3, while the significantly decreased migratory and invasive capacities were observed in the TAB3 inhibition groups (Fig. 3D). Moreover, the increased expression of Vimentin, one of the mesenchymal cell markers, and the reduced expression of the epithelial cell marker, EpCAM, were observed following TAB3 overexpression in the cervical cancer cells. The opposite results, i.e., the decreased expression of Vimentin and the increased expression of EpCAM were observed upon the inhibition of TAB3, suggesting that TAB3 promoted the EMT processes (Fig. 3E). Furthermore, the analyses of p65 expression based on the sub-fraction extracts revealed the increased nuclear p65 and decreased cytoplasmic p65 expression following TAB3 overexpression; opposite results were obtained by the silencing of TAB3 expression in both HeLa and C33A cells (Fig. 3F). The immunofluorescence assays also revealed the enhanced p65 nuclear signals upon TAB3 overexpression in HeLa cells (Fig. 3G and H). RT-qPCR analyses to determine the expression of NF-κB-dependent genes (VEGFB, c-Myc and cyclin D1) revealed their significantly increased expression levels upon TAB3 overexpression, while the silencing of TAB3 decreased their expression levels in HeLa cells (Fig. 3I), suggesting the enhanced nuclear p65 expression and the activation of NF-κB signaling by TAB3 overexpression in cervical cancer cells.

Inhibition of TAB3 abolishes the effects promoted by miR-27a-3p in cervical cancer cells. Since it was observed that miR-27a-3p and TAB3 exerted similar effects on the aggressive phenotypes of cervical cancer cells and that miR-27a-3p promoted the expression of TAB3, the present study therefore determined whether the promoting effects of miR-27a-3p on the malignant potential of cervical cancer cells were achieved due to its promoting effects on TAB3 expression. A series of functional rescue experiments was conducted by co-transfection with miR-27a-3p + shR-TAB3 and ASO-miR-27a-3p + TAB3. As was expected, the elevated colony formation rates induced by miR-27a-3p overexpression were counteracted by the silencing of TAB3 expression, and the suppressed colony formation properties induced by ASO-miR-27a-3p were rescued by TAB3 overexpression in both HeLa and C33A cells (Fig. 4A). The expression levels of EMT-associated specific molecules, i.e., the decreased EpCAM and increased Vimentin expression induced by miR-27a-3p were restored to their normal levels by co-transfection with shR2-TAB3, and vice versa (Fig. 4B). Furthermore, the knockdown of TAB3 mostly abolished the enhanced migratory (Fig. 4C) and invasive (Fig. 4D) abilities of the cervical cancer cells induced by miR-27a-3p overexpression; in addition, the suppressed migratory and invasive properties induced by ASO-miR-27a-3p transfection were counteracted by the ectopic expression of TAB3. The decreased/increased expression of cleaved PARP induced by miR-27a-3p/ASO-miR-27a-3p was also neutralized by the silencing/overexpressing TAB3 expression (Fig. 4E).

Taken together, the findings demonstrated that the suppression of TAB3 at least partially eliminated the effects generated by overexpression miR-27a-3p, and the ectopic expression of TAB3 abolished the effects induced by the inhibition of miR-27a-3p expression, indicating that TAB3 served as a direct functional target gene of miR-27a-3p, and that the enhanced malignant effects induced by miR-27a-3p overexpression were mediated by its promoting effects on TAB3 expression in cervical cancer cells.

The transcription factor p65 directly binds to the promoter region of miR-27a-3p and activates its transcription. Previous studies have reported the dysregulated expression of miR-27a-3p in cervical cancer samples (25,26). In an unpublished screening study by the authors, miR-27a-3p was identified as one of the dysregulated miRNAs by silencing NFKB1 in human cancer cells. The present study thus further focused on the transcriptional regulation of miR-27a-3p, as well as the miR-23a/27a/24-2 cluster. Using bioinformatics analyses, two putative transcription start sites (TSSs) were identified in the analyzed fragment and two promoter reporter vectors containing the two predicted TSSs were constructed, referred to as pGL3-P1 and pGL3-P2, respectively (Fig. 5A). As demonstrated in Fig. S5A, the relative luciferase activity of the fragment P2 was ~4-fold higher than that of the fragment P1, suggesting that the fragment P2 contained the functional promoter sequences. Further analyses of the fragment P2 sequence identified two potential p65 binding sites presented (Fig. 5A, positions: 214-223 and 546-555 in this 773 bp full length) and a series of truncated promoter reporter vectors with none or either one p65 binding site and flanking sequence were constructed, respectively. Of note, the truncated fragments F259 and F509 had higher promoter activities compared with the full-length fragment P2, and both of these only contained the predicted second p65 binding site (position 546-555), suggesting a critical positive regulatory role for this site, while the other one (position 214-223) appeared to have negative effects (Fig. 5B). Following the verification of the efficiencies of the shR-p65 and KBE-p65 vectors (Fig. S5B), the enhanced/decreased promoter activities of fragment P2 and its truncated form F509 were observed upon the modulation of p65 expression (Fig. 5C). Furthermore, this p65 binding site was deleted in fragment F509 and the promoter activities were re-evaluated using dual luciferase reporter systems. As illustrated in Figs. 5C and S5C and D, the significantly decreased promoter activities induced by the silencing of p65 and the silencing of NFKB1 were abolished, and the increased promoter activities induced by the ectopic expression of p65 or NFKB1/p50 were partially decreased, although these were still significantly higher compared with the wild-type sequence of F509 which included the p65 binding site, suggesting the importance of this binding site.

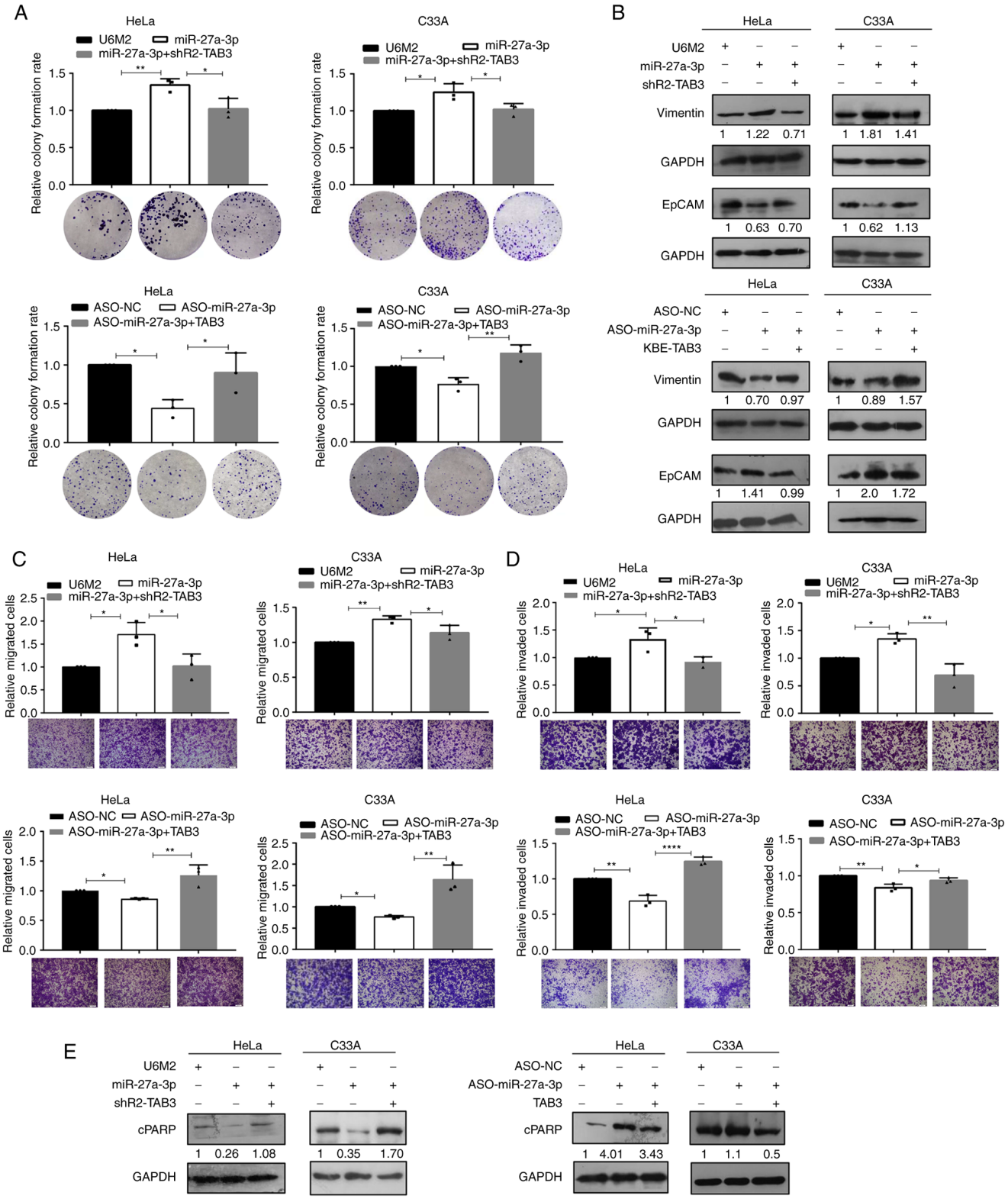

Figure 4. Inhibition of TAB3 abolishes the effects induced by miR-27a-3p in cervical cancer cells. The functional consequences were determined using (A) colony formation assay, (B) western blot analysis for the epithelial-mesenchymal transition specific biomarkers, (C) migration, (D) invasion and (E) apoptosis assays following co-transfection with miR-27a-3p + shR2-TAB3 and ASO-miR-27a-3p + TAB3 to evaluate the functional rescue effects of the miR-27a-3p-induced TAB3 upregulation. (A, C and D) The raw representative graphs of the stained cells are presented under the quantitative histograms; scale bars, 100 μm. (B and E) The numbers under the western blot bands indicate the relative quantifications, as normalized to their endogenous loading control, respectively. *P<0.05, **P<0.01 and ****P<0.0001, vs. their respective control group. TAB3, TGF-β activated kinase 1 binding protein 3.

Furthermore, RT-qPCR assays revealed the increased or decreased primary transcript for this cluster (miR-23a/27a/24-2) and miR-27a-3p expression by p65 overexpression or inhibition, as well as the similar expression patterns for miR-23a-3p and miR-24-2-3p (Fig. 5D), the other two abundant members from the same miRNA cluster,

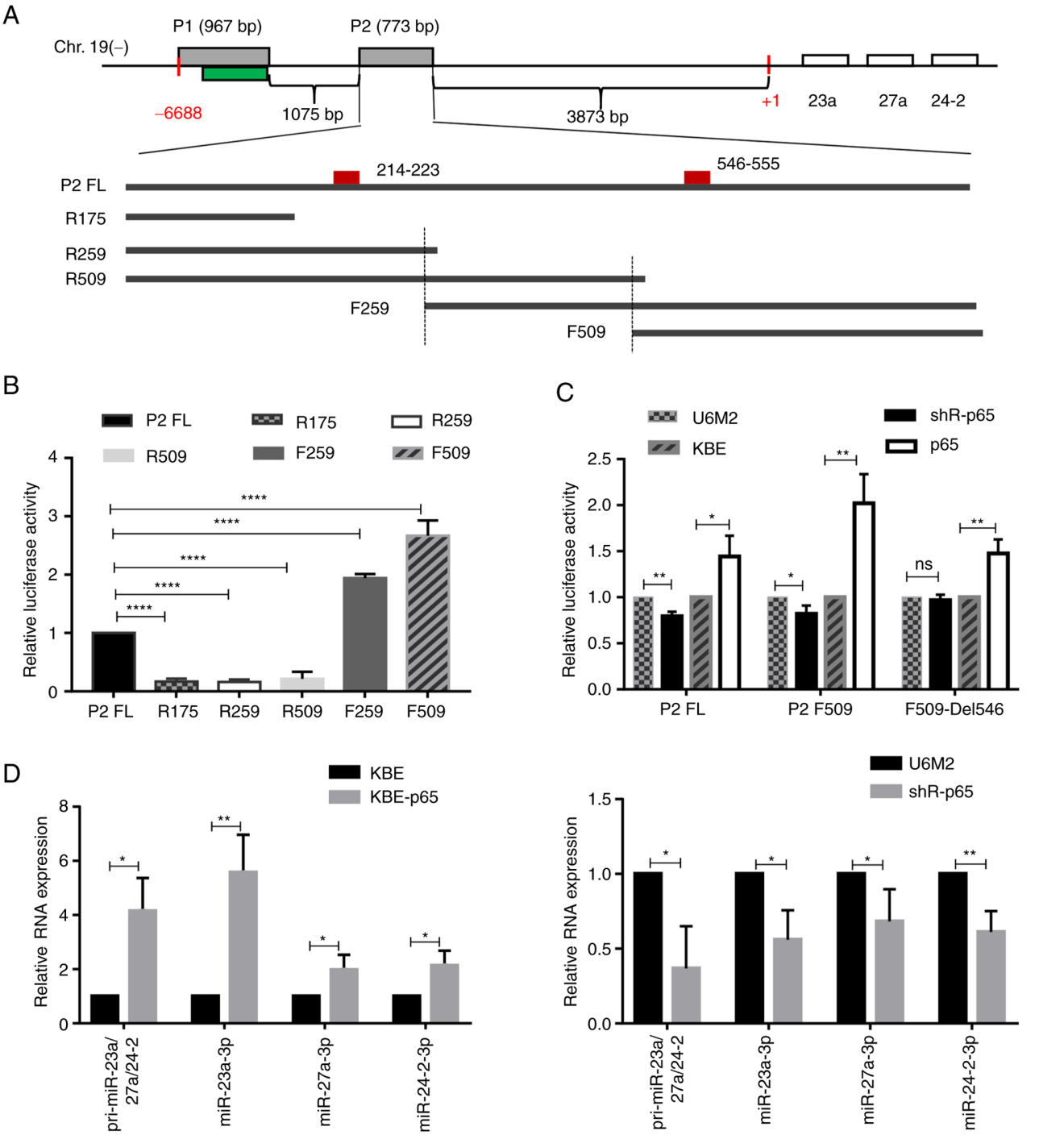

Figure 5. p65 directly binds to the promoter region of miR-27a and activates its transcription. (A) The graph illustrates the location of miR-23a/27a/24-2 cluster and miR-27a-3p in the minus strand of human chromosome 19, as well as the constructed series truncated promoter reporter vectors (P2 full length abbreviated as P2 FL, and the truncated ones, as indicated R175, R259, R509, F259 and F509). The two grey boxes indicate the two amplified fragments (P1 and P2) and the green one indicates the predicted CpG island region. The small red box in the P2 fragment indicates the predicted p65 binding site and their relative positions are labelled with numbers. (B) The relative luciferase activities of the series P2 truncated promoter reporter vectors were determined using dual luciferase reporter systems. (C) The effects of the modulation of p65 expression on the promoter activities of the full length P2, the truncated F509 and the p65 binding site deleted one (F509-Del546). (D) Reverse transcription-quantitative PCR assays were performed to determine the effects of the modulation of p65 expression on the expression levels of pri-miR-23a/27a/24-2, miR-27a-3p, miR-23a-3p and miR-24-2-3p. *P<0.05, **P<0.01 and ****P<0.0001, vs. (B) the P2 Full length group, or (C and D) vs. the respective control group. ns, not significant.

suggesting the members from the same miRNA cluster transcript together. Taken together, these data suggested that the direct binding of p65 to this specific site contributed to the upregulated expression of miR-27a-3p by enhancing its transcription.

Discussion

NF-κB is a transcription factor firstly identified in mature B cells in 1988 (36,37). The mammalian NF-κB family is composed of five members, including RELA/p65, RelB, c-Rel,

NFKB1/p50 and NFKB2/p52. Generally, the heterodimeric complex p50-p65 is the most abundant form of NF-κB in the majority of cells (38). Increasing evidence has indicated that NF-κB is highly activated in a variety of cancer types (39,40). miRNAs not only regulate NF-κB expression directly, but also up- or downregulate NF-κB activity via the upstream or downstream signaling pathways of NF-κB. For example, miR-146a/b can inhibit TRAF6 and IRAK1 expression and further inhibit the NF-κB activity in breast cancer cells (41). miR-1290 was previously found to be upregulated by NF-κB in colon cancer tissues compared with normal adjacent tissues and to directly suppress NF-κB repressing factor, which in turn activated the Akt and NF-κB pathways (42). The present study first investigated the functional effects of miR-27a-3p, one of the identified dysregulated miRNAs by silencing NFKB1, and further investigated its regulatory roles in cervical cancer cells. Using bioinformatics analyses and experimental validation, it was found that miR-27a-3p upregulated TAB3 expression by binding to its 3'UTR and subsequently triggered the activation of NF-κB signaling. Functionally, it was demonstrated that miR-27a-3p promoted the malignant potential of cervical cancer cells, and rescue experiments suggested that the enhanced malignant potential induced by miR-27a-3p overexpression was directly mediated by its upregulation of TAB3.

As a class of non-coding RNA molecules, the functions of miRNAs have been extensively studied in various cancer types over the past decade, while the mechanisms responsible for their dysregulated expression remain to be fully elucidated. It has been reported that the miR-203 locus is highly methylated and epigenetically silenced by DNA methylation in several metastatic tumor cells (16,17). Ma *et al* (43) demonstrated a positive feedback loop composed of KLF3, miR-23a/27a, β-like globin gene and the miR-23a/27a/24-2 cluster during erythropoiesis. In addition, another study demonstrated that c-Fos transcriptionally activated miR-27a expression and miR-27a regulated the translocation of apoptosis-inducing factor from the mitochondria to the nucleus by targeting ATAD3a and contributed to myocardial ischemia-reperfusion injury (44). Tao *et al* (45) concluded that the transcription factor p53 significantly decreased the expression of miR-27a by binding to the specific sites of the promoter region in mouse ovarian granulosa cells. The present study identified one specific p65 binding site in the promoter region of the miR-23a/27a/24-2 cluster, and p65 transcriptionally enhanced the expression levels of primary miRNA transcript and mature miRNAs, while the silencing of p65 significantly decreased their expression levels in cervical cancer cells. In particular, it was found that NFKB1/p50 had similar effects as p65, although no p50 binding site was present in the reporter construct, which was reasonable and explainable, since the p50-p65 heterodimer was the most abundant form of the NF-κB transcription factor. Moreover, as an upstream activator of the NF-κB pathway, TAB3 was also upregulated by miR-27a-3p and enhanced the nuclear translocation of the p65-p50 heterodimer, suggesting the positive feedback loop among miR-27a-3p, TAB3 and the NF-κB signaling pathway.

In recent years, several studies have presented controversial functional results on miR-27a in cervical cancer cells, and indicated its oncogenic or tumor suppressor roles in different situations. For example, as previously demonstrated, miR-27a-3p plays an oncogenic functional role by promoting the proliferation, migration and invasion of HeLa cells, mediated by the inhibition of BTG2 and FBXW7 expression using miR-27a-3p mimic individually (24,26). However, Fang *et al* (25) reported that miR-27a-3p overexpression using Agomir (chemically modified miRNA mimic) inhibited the proliferation, migration and invasion of HeLa cells by downregulating TGF-βRI. The present study investigated the functional effects of miR-27a-3p using the strand specific expression vector in both the cervical adenocarcinoma cell line, HeLa, and the cervical squamous cell carcinoma cell line, C33A. Compared with the traditional construction method for miRNA overexpression, in which both -3p and -5p are expressed together, the current strand specific expression construct can only produce the indicated miR-27a-3p molecule. The results suggested the oncogenic roles of miR-27a-3p in both HeLa and C33A cells by promoting the colony formation, migratory and invasive abilities upon the overexpression of miR-27a-3p.

Typically, miRNAs negatively regulate multiple genes and lead to mRNA degradation or translation suppression via binding to the 3'UTRs (46). Some studies have also shown the positive regulation of gene expression by miRNAs. For example, a previous study demonstrated that miR-744 upregulated CCNB1 expression by promoting the enrichment of RNA polymerase II and the tri-methylation of histone 3 at lysine 4 (H3K4me3) at its transcription start site in mouse NIH/3T3 cells (47). Another study demonstrated that miR-122 enhanced hepatitis C virus (HCV) replication by targeting its 5'-noncoding elements in the HCV genome (48). In addition, it was previously found that miR-1 exerted inhibitory effects in the cytoplasm, while it stimulated the translation of mitochondrial genome-encoded ND1 and COX1 when GW182 was silenced in the cytoplasm (49). Song *et al* (50) reported that miR-346 bound to the 3'UTR of hTERT and upregulated its expression by recruiting the mRNA to the ribosome and promoted its translation in an AGO2-independent manner, which was mediated by G-rich RNA sequence binding factor 1 (GRSF1). In the present study, the enhanced expression of TAB3 was observed following the overexpression of miR-27a-3p and this enhancement may be at least partially mediated in an AGO2-dependent manner, since similar upregulated TAB3 expression patterns (miR-27a-3p vs. control) were observed following the silencing of AGO2. However, whether other proteins, such as GRSF1 are also involved in the promoting effects remains unclear. The transfected HeLa cells were further treated with cycloheximide and actinomycin D individually, and the stabilities of TAB3 were determined; no significant differences were observed in the presence of altering miR-27a-3p expression, which indicated that the upregulated TAB3 expression induced by miR-27a-3p was not due to the increased protein stability or the cessative transcription activity (data not shown). It was thus hypothesized that this upregulation may probably resulted from the enhanced synthesis of transcripts. However, further mechanistic analyses are required for further clarifications.

Of note, the globally decreased endogenous expression of TAB3 was observed following the silencing of AGO2 expression with/without miR-27a-3p overexpression in cervical cancer cells. AGO2 may be involved in the inhibition of translation initiation either by binding to the 7-methylguanosine cap (51) or via the interaction with eIF6 and preventing the assembly

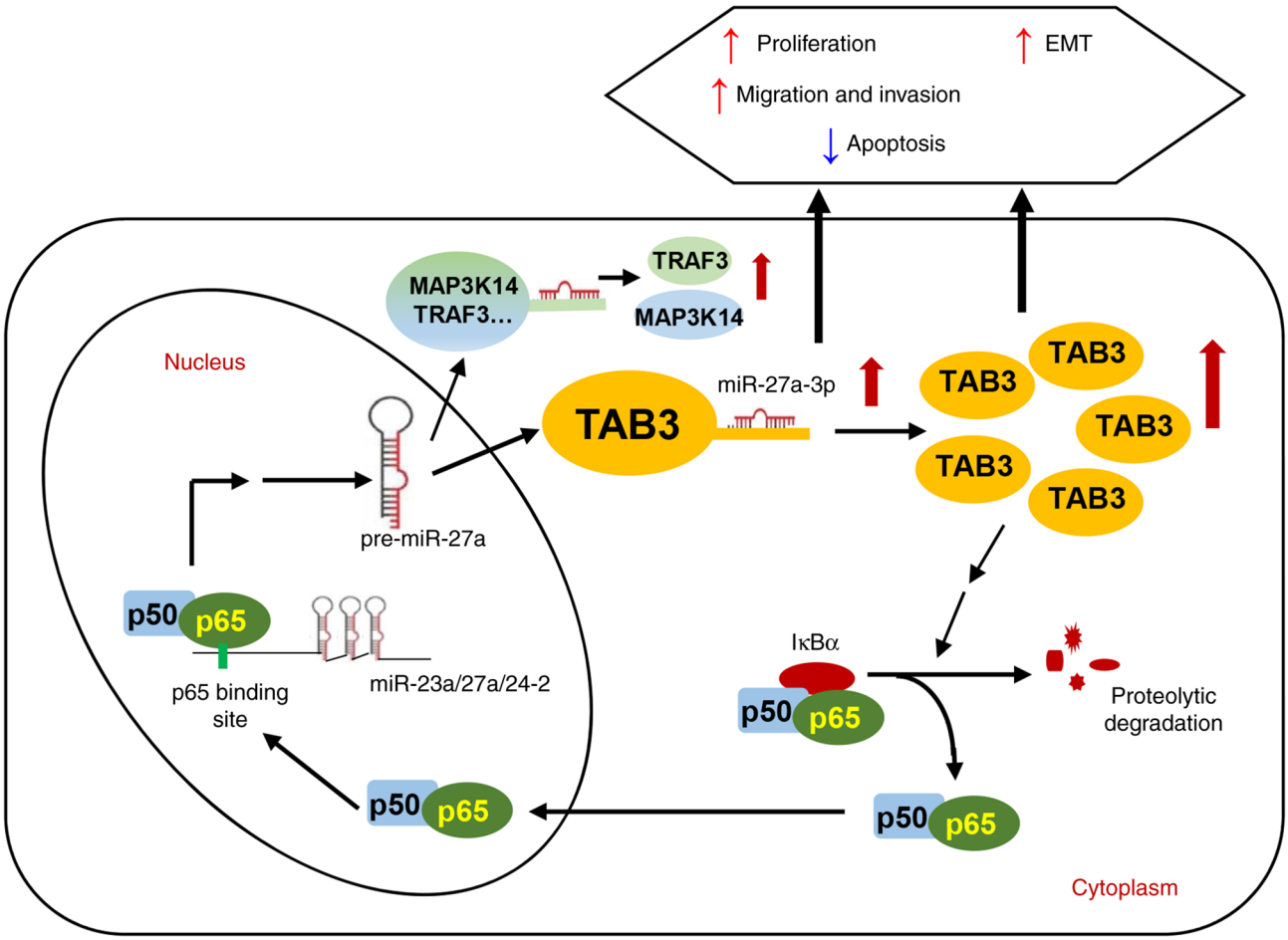

Figure 6. Models of the positive regulatory feedback loop of p65/miR-27a-3p/TAB3/NF-κB axis. Transcriptionally activation of miR-27a-3p by p65 overexpression enhanced TAB3 expression, and subsequently activated the NF-κB signaling pathway and is involved in the malignant potential of cervical cancer cells, which presents the positive feedback regulatory loop and its involvement in cervical tumorigenesis. TAB3, TGF-β activated kinase 1 binding protein 3; EMT, epithelial-mesenchymal transition; TRAF3, TNF receptor associated factor 3; MAP3K14, mitogen-activated protein kinase kinase kinase 14.

of ribosome (52), further resulting in mRNA degradation in the processing bodies (P-bodies). This may be a reasonable explanation for the globally decreased TAB3 protein expression by inhibiting AGO2. On the other hand, the AGO2 protein is required for RNA-mediated gene silencing by the RNA-induced silencing complex. According to the miRTarBase prediction, 18 miRNAs were predicted to target TAB3 in total, and some miRNAs were verified in experimental systems (53,54). Thus, it can be hypothesized that the silencing of AGO2 may affect the miRNA-mediated regulatory effects on TAB3, which may also result in the globally reduced expression of TAB3. However, further experimental evidence is required to answer this question precisely and this may represent another challenging research topic for the future.

Moreover, TRAF3 and MAP3K14 were also identified and verified as direct targets of miR-27a-3p using EGFP 3'UTR reporters, RT-qPCR and western blot analyses in the present study. Among these, MAP3K14 could bind to TRAF2 and stimulate NF-κB activity, while TRAF3 functioned as a constitutive negative regulator of the alternative NF-κB pathway. Taken together, it can be hypothesized that the effects induced by miR-27a-3p on NF-κB activities not only derived from its upregulation of TAB3, but may also be attributed to other molecules involved in the NF-κB signaling pathway, such as MAP3K14 and TRAF3 presented herein. It may be of interest to formulate the miR-27a-3p and NF-κB signaling pathway-associated regulatory network.

In conclusion, the present study revealed that NF-κB/p65 transcriptionally activated miR-27a-3p and miR-27a-3p promoted TAB3 expression by binding to its 3'UTR and subsequently activated the NF-κB signaling pathway, which contributed to cervical tumorigenesis. Functionally, it was demonstrated that miR-27a-3p enhanced the colony formation, migratory and invasive abilities of cervical cancer cells and promoted the EMT process. Moreover, TAB3 played an oncogenic role and functional rescue experiments indicated that the oncogenic functions induced by miR-27a-3p were mediated by its upregulation of TAB3 expression in cervical cancer cells. In addition, the miR-27a-3p upstream transcription factor, p65, was identified to promote the transcription and expression of the miR-23a/27a/24-2 cluster members. Taken together, the present study demonstrated a positive feedback regulatory loop composed of p65, miR-27a-3p, TAB3 and the NF-κB pathway in the progression of cervical cancer (Fig. 6), suggesting a novel miRNA-mediated mechanism between pro-inflammation and tumor transformation by the continuous activation of the NF-κB pathway. A limitation of the present study was lack of *in vivo* evaluations, while

studies from other groups have also indicated the oncogenic roles of miR-27a-3p in cervical cancer cells (21,23), which may function as a supplement to the *in vitro* experiments herein. The present study highlighted the oncogenic roles of TAB3 and miR-27a-3p in cervical cancer cells, which may provide new insight into cervical cancer malignancies, and may provide potential valuable novel biomarkers for clinical applications.

Acknowledgements

The authors would like to thank Dr Weiying Liu and Dr Qi Sun from Tianjin Medical University for providing the KBE-p65, KBE-p50 vectors and shR-NFKB1 vector, and Dr Per Johansson from Karolinska Institutet for providing the pcDNA3-U6M2 vector.

Funding

The present study was supported by the National Natural Science Foundation of China (grant nos. 81773002 and 31971100) and the Natural Science Foundation of Tianjin City (grant no. 16JCYBJC42400).

Availability of data and materials

The datasets used and analyzed during the current study are available from the corresponding author on reasonable request.

Authors' contributions

HX conceived, designed and supervised the study. HX, ML, ZG and SW performed the experiments. HX, ML, ZG, SW and YZ analyzed and interpreted the data. ML, YZ and HX wrote the manuscript. ML and HX confirm the authenticity of all the raw data. All authors provided comments, and have read and approved the final manuscript.

Ethics approval and consent to participate

Not applicable.

Patient consent for publication

Not applicable.

Competing interests

The authors declare that they have no competing interests.

References

1. Sung H, Ferlay J, Siegel RL, Laversanne M, Soerjomataram I, Jemal A and Bray F: Global Cancer Statistics 2020: GLOBOCAN estimates of incidence and mortality worldwide for 36 cancers in 185 countries. CA Cancer J Clin 71: 209-249, 2021.
2. zur Hausen H: Papillomaviruses in the causation of human cancers-a brief historical account. Virology 384: 260-265, 2009.
3. Scarth JA, Patterson MR, Morgan EL and Macdonald A: The human papillomavirus oncoproteins: A review of the host pathways targeted on the road to transformation. J Gen Virol 102: 001540, 2021.
4. Liang LA, Einzmann T, Franzen A, Schwarzer K, Schauberger G, Schriefer D, Radde K, Zeissig SR, Ikenberg H, Meijer CJLM, *et al*: Cervical cancer screening: Comparison of conventional pap smear test, liquid-based cytology, and human papillomavirus testing as stand-alone or Cotesting strategies. Cancer Epidemiol Biomarkers Prev 30: 474-484, 2021.
5. Perkins RB, Guido RL, Saraiya M, Sawaya GF, Wentzensen N, Schiffman M and Feldman S: Summary of current guidelines for cervical cancer screening and management of abnormal test results: 2016-2020. J Womens Health (Larchmt) 30: 5-13, 2021.
6. Lei J, Ploner A, Elfström KM, Wang J, Roth A, Fang F, Sundström K, Dillner J and Sparén P: HPV Vaccination and the risk of invasive cervical cancer. N Engl J Med 383: 1340-1348, 2020.
7. Palmer T, Wallace L, Pollock KG, Cuschieri K, Robertson C, Kavanagh K and Cruickshank M: Prevalence of cervical disease at age 20 after immunisation with bivalent HPV vaccine at age 12-13 in Scotland: Retrospective population study. BMJ 365: l1161, 2019.
8. Farazi TA, Hoell JI, Morozov P and Tuschl T: MicroRNAs in Human Cancer. In: MicroRNA Cancer Regulation. pp1-20, 2013.
9. He Y, Lin J, Ding Y, Liu G, Luo Y, Huang M, Xu C, Kim TK, Etheridge A, Lin M, *et al*: A systematic study on dysregulated microRNAs in cervical cancer development. Int J Cancer 138: 1312-1327, 2016.
10. Lui WO, Pourmand N, Patterson BK and Fire A: Patterns of known and novel small rnas in human cervical cancer. Cancer Res 67: 6031-6043, 2007.
11. Xie H, Zhao YG, Caramuta S, Larsson C and Lui WO: miR-205 expression promotes cell proliferation and migration of human cervical cancer cells. PLoS One 7: e46990, 2012.
12. Xie H, Lee L, Scicluna P, Kavak E, Larsson C, Sandberg R and Lui WO: Novel functions and targets of miR-944 in human cervical cancer cells. Int J Cancer 136: E230-E241, 2015.
13. Calin GA, Dumitru CD, Shimizu M, Bichi R, Zupo S, Noch E, Aldler H, Rattan S, Keating M, Rai K, *et al*: Frequent deletions and down-regulation of micro-RNA genes miR15 and miR16 at 13q14 in chronic lymphocytic leukemia. Proc Natl Acad Sci USA 99: 15524-15529, 2002.
14. Jin HY, Oda H, Lai M, Skalsky RL, Bethel K, Shepherd J, Kang SG, Liu WH, Sabouri-Ghomi M, Cullen BR, *et al*: MicroRNA-17~92 plays a causative role in lymphomagenesis by coordinating multiple oncogenic pathways. EMBO J 32: 2377-2391, 2013.
15. Feng Y, Zhou S, Li G, Hu C, Zou W, Zhang H and Sun L: Nuclear factor-κB-dependent microRNA-130a upregulation promotes cervical cancer cell growth by targeting phosphatase and tensin homolog. Arch Biochem Biophys 598: 57-65, 2016.
16. Bueno MJ, Pérez de Castro I, Gómez de Cedrón M, Santos J, Calin GA, Cigudosa JC, Croce CM, Fernández-Piqueras J and Malumbres M: Genetic and epigenetic silencing of MicroRNA-203 enhances ABL1 and BCR-ABL1 oncogene expression. Cancer Cell 13: 496-506, 2008.
17. Cui X, Chen X, Wang W, Chang A, Yang L, Liu C, Peng H, Wei Y, Liang W, Li S, *et al*: Epigenetic silencing of miR-203 in Kazakh patients with esophageal squamous cell carcinoma by MassARRAY spectrometry. Epigenetics 12: 698-707, 2017.
18. Yang Y, Yang Z, Zhang R, Jia C, Mao R, Mahati S, Zhang Y, Wu G, Sun YN, Jia XY, *et al*: MiR-27a-3p enhances the cisplatin sensitivity in hepatocellular carcinoma cells through inhibiting PI3K/Akt pathway. Biosci Rep 41: BSR20192007, 2021.
19. Chae DK, Ban E, Yoo YS, Kim EE, Baik JH and Song EJ: MIR-27a regulates the TGF-signaling pathway by targeting SMAD2 and SMAD4 in lung cancer. Mol Carcinogen 56: 1992-1998, 2017.
20. Kong LY, Xue M, Zhang QC and Su CF: In vivo and in vitro effects of microRNA-27a on proliferation, migration and invasion of breast cancer cells through targeting of SFRP1 gene via Wnt/β-catenin signaling pathway. Oncotarget 8: 15507-15519, 2017.
21. Liang JT, Tang JM, Shi HJ, Li H, Zhen T, Duan J, Kang L, Zhang F, Dong Y and Han A: miR-27a-3p targeting RXR α promotes colorectal cancer progression by activating Wnt/β-catenin pathway. Oncotarget 8: 82991-83008, 2017.
22. You J, Li J, Ke C, Xiao Y, Lu C, Huang F, Mi Y, Xia R and Li Q: Oncogenic long intervening noncoding RNA Linc00284 promotes c-Met expression by sponging miR-27a in colorectal cancer. Oncogene 40: 4151-4166, 2021.

23. Shi J, Yang C, An J, Hao D, Liu C, Liu J, Sun J and Jiang J: KLF5-induced BBOX1-AS1 contributes to cell malignant phenotypes in non-small cell lung cancer via sponging miR-27a-5p to up-regulate MELK and activate FAK signaling pathway. J Exp Clin Cancer Res 40: 148, 2021.
24. Li S, Han Y, Liang X and Zhao M: LINC01089 inhibits the progression of cervical cancer via inhibiting miR-27a-3p and increasing BTG2. J Gene Med 23: e3280, 2020.
25. Fang F, Huang B, Sun S, Xiao M, Guo J, Yi X, Cai J and Wang Z: miR-27a inhibits cervical adenocarcinoma progression by down-regulating the TGF-βRI signaling pathway. Cell Death Dis 9: 395, 2018.
26. Ben W, Zhang G, Huang Y and Sun Y: MiR-27a-3p regulated the aggressive phenotypes of cervical cancer by targeting FBXW7. Cancer Manag Res 12: 2925-2935, 2020.
27. Jin G, Klika A, Callahan M, Faga B, Danzig J, Jiang Z, Li X, Stark GR, Harrington J and Sherf B: Identification of a human NF-kappa B-activating protein, TAB3. Proc Natl Acad Sci USA 101: 2028-2033, 2004.
28. Cheung PCF, Nebreda AR and Cohen P: TAB3, a new binding partner of the protein kinase TAK1. Biochem J 378: 27-34, 2004.
29. Li Q, Chen L, Luo C, ChenYan, Ge J, Zhu Z, Wang K, Yu X, Lei J, Liu T, *et al*: TAB3 upregulates PIM1 expression by directly activating the TAK1-STAT3 complex to promote colorectal cancer growth. Exp Cell Res 391: 111975, 2020.
30. Zhao J, Gai L, Gao Y, Xia W, Shen D, Lin Q, Mao W, Wang F, Liu P, Chen J, *et al*: TAB3 promotes human esophageal squamous cell carcinoma proliferation and invasion via the NF-κB pathway. Oncol Rep 40: 2876-2885, 2018.
31. Chen Y, Wang X, Duan C, Chen J, Su M, Jin Y, Deng Y, Wang D, Chen C, Zhou L, *et al*: Loss of TAB3 expression by shRNA exhibits suppressive bioactivity and increased chemical sensitivity of ovarian cancer cell lines via the NF-B pathway. Cell Prolif 49: 657-668, 2016.
32. Luo C, Yuan R, Chen L, Zhou W, Shen W, Qiu Y, Shao J, Yan J and Shao J: TAB3 upregulates Survivin expression to promote colorectal cancer invasion and metastasis by binding to the TAK1-TRAF6 complex. Oncotarget 8: 106565-106576, 2017.
33. Ding J, Huang S, Wang Y, Tian Q, Zha R, Shi H, Wang Q, Ge C, Chen T, Zhao Y, *et al*: Genome-wide screening reveals that miR-195 targets the TNF-α/NF-κB pathway by down-regulating IκB kinase alpha and TAB3 in hepatocellular carcinoma. Hepatology 58: 654-666, 2013.
34. Kumar S, Xie H, Shi H, Gao J, Juhlin CC, Björnhagen V, Höög A, Lee L, Larsson C and Lui WO: Merkel cell polyomavirus oncoproteins induce microRNAs that suppress multiple autophagy genes. Int J Cancer 146: 1652-1666, 2020.
35. Livak KJ and Schmittgen TD: Analysis of relative gene expression data using real-time quantitative PCR and the 2(-Delta Delta C(T)) method. Method 25: 402-408, 2001.
36. Baeuerle PA and Baltimore D: Activation of DNA-binding activity in an apparently cytoplasmic precursor of the NF-kappa B transcription factor. Cell 53: 211-217, 1988.
37. Baeuerle PA and Baltimore D: I kappa B: A Specific Inhibitor of the NF-kappa B Transcription Factor. Science 242: 540-546, 1988.
38. Karin M, Yamamoto Y and Wang QM: The IKK NF-kappaB system: A treasure trove for drug development. Nat Rev Drug Discov 3: 17-26, 2004.
39. Biswas DK, Shi Q, Baily S, Strickland I, Ghosh S, Pardee AB and Iglehart JD: NF-kappa B activation in human breast cancer specimens and its role in cell proliferation and apoptosis. Proc Natl Acad Sci USA 101: 10137-10142, 2004.
40. Sakamoto K, Maeda S, Hikiba Y, Nakagawa H, Hayakawa Y, Shibata W, Yanai A, Ogura K and Omata M: Constitutive NF-kappa B activation in colorectal carcinoma plays a key role in angiogenesis, promoting tumor growth. Clin Cancer Res 15: 2248-2258, 2009.
41. Bhaumik D, Scott GK, Schokrpur S, Patil CK, Campisi J and Benz CC: Expression of microRNA-146 suppresses NF-kappaB activity with reduction of metastatic potential in breast cancer cells. Oncogene 27: 5643-5647, 2008.
42. Wu J, Ji X, Zhu L, Jiang Q, Wen Z, Xu S, Shao W, Cai J, Du Q, Zhu Y and Mao J: Up-regulation of microRNA-1290 impairs cytokinesis and affects the reprogramming of colon cancer cells. Cancer Lett 329: 155-163, 2013.
43. Ma Y, Wang B, Jiang F, Wang D, Liu H, Yan Y, Dong H, Wang F, Gong B, Zhu Y, *et al*: A feedback loop consisting of MicroRNA 23a/27a and the β-Like globin suppressors KLF3 and SP1 regulates globin gene expression. Mol Cell Biol 33: 3994-4007, 2013.
44. Bao YD, Qiao Y, Yu H, Zhang Z, Yang H, Xin X, Chen Y, Guo Y, Wu N and Jia D: miRNA-27a transcription activated by c-Fos regulates myocardial ischemia-reperfusion injury by targeting ATAD3a. Oxid Med Cell Longev 2021: 2514947, 2021.
45. Tao H, Xiong Q, Ji Z, Zhang F, Liu Y and Chen M: NFAT5 is Regulated by p53/miR-27a Signal axis and promotes mouse ovarian granulosa cells proliferation. Int J Biol Sci 15: 287-297, 2019.
46. Meijer HA, Kong YW, Lu WT, Wilczynska A, Spriggs RV, Robinson SW, Godfrey JD, Willis AE and Bushell M: Translational repression and eIF4A2 activity are critical for MicroRNA-Mediated gene regulation. Science 340: 82-85, 2013.
47. Huang V, Place RF, Portnoy V, Wang J, Qi Z, Jia Z, Yu A, Shuman M, Yu J and Li LC: Upregulation of Cyclin B1 by miRNA and its implications in cancer. Nucleic Acids Res 40: 1695-1707, 2012.
48. Roberts APE, Lewis AP and Jopling CL: miR-122 activates hepatitis C virus translation by a specialized mechanism requiring particular RNA components. Nucleic Acids Res 39: 7716-7729, 2011.
49. Zhang X, Zuo X, Yang B, Li Z, Xue Y, Zhou Y, Huang J, Zhao X, Zhou J, Yan Y, *et al*: MicroRNA directly enhances mitochondrial translation during muscle differentiation. Cell 158: 607-619, 2014.
50. Song G, Wang R, Guo J, Liu X, Wang F, Qi Y, Wan H, Liu M, Li X and Tang H: miR-346 and miR-138 competitively regulate hTERT in GRSF1- and AGO2-dependent manners, respectively. Sci Rep 5: 15793, 2015.
51. Kiriakidou M, Tan GS, Lamprinaki S, De Planell-Saguer M, Nelson PT and Mourelatos Z: An mRNA m7G cap binding-like motif within human Ago2 represses translation. Cell 129: 1141-1151, 2007.
52. Chendrimada TP, Finn KJ, Ji XJ, Baillat D, Gregory RI, Liebhaber SA, Pasquinelli AE and Shiekhattar R: MicroRNA silencing through RISC recruitment of eIF6. Nature 447: 823-821, 2007.
53. Jiang L, Yu L, Zhang X, Lei F, Wang L, Liu X, Wu S, Zhu J, Wu G, Cao L, *et al*: miR-892b silencing activates NF-κB and promotes aggressiveness in breast cancer. Cancer Res 76: 1101-1111, 2016.
54. Zhou X, Chen JJ, Zhang HJ, Chen X and Shao GH: MicroRNA-23b attenuates the H_2O_2-induced injury of microglial cells via TAB3/NF-κB signaling pathway. Int J Clin Exp Pathol 11: 5765-5773, 2018.